Transition from Amorphous Semiconductor to Amorphous Insulator in Hydrogenated Carbon−Germanium Films Investigated by Raman Spectroscopy

P. Kazimierski and J. Tyczkowski*

Technical University of Lodz, Faculty of Process and Environmental Engineering, 93-005 Lodz, Wolczanska 213, Poland

M. Kozanecki

Technical University of Lodz, Faculty of Chemistry, 90-924 Lodz, Zeromskiego 116, Poland

Y. Hatanaka and T. Aoki

Research Institute of Electronics, Shizuoka University, 3-5-1 Johoku, Hamamatsu 432, Japan

Received April 30, 2002. Revised Manuscript Received July 23, 2002

Amorphous hydrogenated carbon−germanium films (a-Ge_XC_Y:H) were fabricated by plasma chemical vapor deposition in an audio frequency (af) three-electrode reactor using tetramethylgermane (TMGe) as a source compound. Two types of the material, namely semiconducting (a-S) and insulating (a-I) films characterized by quite different electronic properties, were produced. For example, electrical conductivity at room temperature, T_{room}, amounts to approximately 10^{-18} S/m (with activation energy $E_A \approx 0.9$ eV) and 10^{-4} S/m ($E_A \approx 0.3$ eV) for a-I and a-S, respectively. This very drastic change in the electronic structure of the a-Ge_XC_Y:H films can be caused by a very small variation of the plasma deposition conditions and therefore it is termed a-I−a-S transition. The previous attempts to explain the nature of the a-I−a-S transition from the molecular and supermolecular point of view (quantitative chemical microanalysis, XPS and IR spectrscopies, TEM, SEM, electron diffraction, and AFM) have failed. In this paper Raman spectroscopy has been used to this end. It has been found that the carbon structure does not determine the electronic properties of the films and sp^2 sites are not responsible for the a-I−a-S transition. This conclusion is supported by investigations on a-Ge_XC_Y:H films, in which sp^2 sites are purposely created. On the other hand, a drastic difference in the Ge atoms dispersion in the a-I and a-S has been found. In the a-I films a great amount of Ge atoms is molecularly dispersed, whereas in the a-S films the vast majority of Ge atoms is in the form of a-Ge several-nanometer-sized clusters. It is suggested that these clusters play a crucial role in the formation of the amorphous semiconductor network and they are responsible for the a-I−a-S transition.

Introduction

It has been found that hydrogenated carbon−germanium films (a-Ge_XC_Y:H) plasma deposited from a single precursor (e.g. tetramethylgermane) can exist in one of two distinct electronic structures, depending on deposition conditions.[1] These two qualitatively different kinds of material, namely amorphous semiconductor (a-S) and amorphous insulator (a-I), are characterized, for example, by values of specific electrical conductivity on the order of 10^{-4} and 10^{-18} S/m, respectively. Also their optical gap reflects a transformation in the electronic structure and a shift from 3.2 eV for a-I to 2.0 eV for a-S samples is observed. This very drastic change in the electronic structure (a-I−a-S transition) can be caused by a very small variation of the plasma deposition conditions that are responsible for the impact energy of ions bombarding the growing film.[2]

It has been highly interesting to find out how the change in the electronic structure of a-Ge_XC_Y:H films is controlled by the chemical structure. Detailed investigations on quantitative chemical microanalysis and XPS revealed that the differences between a-S and a-I forms could not be attributed to changes in the elemental composition of these materials.[3,4] More details on the chemical structure were obtained from IR spectroscopy. Although it was clearly shown that a-S samples were more cross-linked, no rapid changes in the chemical structure between a-S and a-I, contrary to their electronic structure, were also observed.[3] Similarly, inves-

(1) Tyczkowski, J.; Kazimierski, P. *J. Phys. D: Appl. Phys.* **1994**, *27*, 179.

(2) Tyczkowski, J. *J. Vac. Sci. Technol. A* **1999**, *17*, 470.

(3) Tyczkowski, J.; Kazimierski, P.; Szymanowski, H. *Thin Solid Films* **1993**, *241*, 291.

(4) Kazimierski, P.; Tyczkowski, J.; Delamar, M.; Lehmberg, H. *J. Non-Cryst. Solids* **1998**, *227/230*, 422.

10.1021/cm020428s CCC: $22.00
Published on Web 10/18/2002

tigations performed by the transmission (TEM) and scanning (SEM) electron microscopy as well as by the electron diffraction have not revealed any differences in the supermolecular structure between the a-I and a-S films.[5] A certain confirmation of the a-I−a-S transition, from the supermolecular structure point of view, has been given, however, by the atomic force microscopy (ATM) and unconventional analysis of XPS spectra.[4] These measurements indicate that a-Ge_XC_Y:H films have a nonhomogeneous distribution of charge that step changes between the a-I and a-S forms. Unfortunately, the chemical nature of the transition is still unclear.

Two facts, namely the first that the a-S−a-I transition has been found not only for a-Ge_XC_Y:H but recently also for other related films, e.g. a-Si_XC_Y:H,[6] a-Sn_XC_Y:H,[7] a-Pb_XC_Y:H,[8] and the second that the carbon content in all these films is very high (70−85 mol %), impose the necessity to verify whether the effect is not, by any chance, a result of specific changes only in the carbon structure of the films.

It is widely recognized that the ion impact energy during deposition of hydrogenated carbon films (a−C:H) is the most important deposition parameter. By a variation of the impact energy the properties of a-C:H can be varied over a wide range. Ion bombardment affects primarily the hydrogen content. Increasing the impact energy reduces the hydrogen incorporation. As a result, the degree of three-dimensional cross-linking realized by C−C bonds grows in the hydrocarbon network. Further increase in the impact energy causes creation of graphitic clusters, and with the energy the fraction of graphite (sp^2) versus tetrahedral (sp^3) bonding increases. Thus, the films are very polymeric at low impact energy, diamondlike at intermediate ion energies, and quite graphitic at high values of the energy.[9] As a consequence, the optical gap of the films decreases and their conductivity increases with growing ion impact energy. For intermediate and high values of the energy, the optical gap can change from 2.7 to 1.0 eV, and the conductivity from 10^{-13} to 10^2 S/ m.[9−15] These differences, which are commonly attributed to sp^2 sites, resemble those characteristic of the a-I and a-S forms of the a-Ge_XC_Y:H films under discussion.

On the other hand, thorough investigations performed on a-C:H films deposited from pentane in the same reactor and under similar conditions in which a-Ge_XC_Y:H films revealing the a-I−a-S transition were fabricated have shown that there is no data indicative of the effect in this case.[16] Nevertheless, the connection of the transition only with carbon network should not be disregarded, and the question whether the existence of a-I and a-S forms can be explained only by changes in the carbon network in which sp^2 sites are created or it is more complex phenomenon is still open. In this paper we undertake an attempt to solve this problem on the basis of Raman studies.

Raman spectroscopy is an especially useful nondestructive method to distinguish and analyze carbon structures. It is easy, for example, to identify graphite (sp^2) and diamond (sp^3) crystals, because the zone-center optical phonons in these structures occur at well-separated frequencies of 1580 and 1332 cm^{-1}, respectively.[17] For amorphous carbon films, however, Raman studies, which are mainly performed using visible laser excitation at 488 or 514 nm, allow, in principle, the identification only of sp^2 sites. This is a result of a much larger Raman cross section for sp^2 sites in comparison with sp^3 sites. Even when the sp^3 fraction exceeds 80%, it is not revealed by visible Raman spectra.[18] We can observe, however, the vibrational mode of sp^3-bonded carbon as a wide peak (termed the *T* peak) at approximately 1100 cm^{-1} if we use UV−Raman spectroscopy with 244 nm excitation, which has been very recently shown.[18−21]

In general, visible Raman spectra of amorphous hydrogenated carbon films (a-C:H) show two characteristic peaks corresponding to the typical graphite G line centered at around 1580 cm^{-1} and the so-called disordered graphite D line centered around 1350 cm^{-1}.[18,22−25] It is widely recognized that the former line originates from lattice vibrations in the plane of the graphite-like rings, whereas the latter line results from the disorder-allowed zone-edge mode of graphite clusters. It is suggested, however, that these lines can be also associated with isolated benzene or condensed benzene rings. Moreover, the G line may even be formed by olefinic sp^2 bonds alone.[22,26]

In some cases, when amorphous films containing carbon atoms are deposited on a cold substrate (up to ca. 450 K), a broad line in the region of 1400−1500 cm^{-1} occurs. This line has been observed both for amorphous carbon (hydrogenated and non-hydrogenated) films[22,24,27] and more complex systems such as carbon−silicon[28] and

(5) Tyczkowski, J.; Pietrzyk, B.; Mazurczyk, R.; Polański, K.; Balcerski, J.; Delamar, M. *Appl. Phys. Lett.* **1997**, *71*, 2943.
(6) Tyczkowski, J.; Pietrzyk, B.; Kazimierski, P.; Gubiec, K. *Surf. Coat. Technol.* **2001**, *142/144*, 843.
(7) Tyczkowski, J.; Pietrzyk, B.; Hatanaka, Y.; Nakanishi, Y. *Appl. Surf. Sci.* **1997**, *113/114*, 534.
(8) Tyczkowski, J.; Pietrzyk, B.; Delamar, M. *Chem. Mater.* **1998**, *10*, 3879.
(9) Robertson, J. *Diamond Relat. Mater.* **1994**, *3*, 361.
(10) Robertson, J. *Adv. Phys.* **1986**, *35*, 317.
(11) Weissmantel, S.; Bewilogua, K.; Dietrich, D.; Erler, H. J.; Hinneberg, H. J.; Klose, S.; Nowick, W.; Reisse, G. *Thin Solid Films* **1980**, *72*, 19.
(12) Natarajan, V.; Lamb, J. D.; Woollam, J. A.; Liu, D. C.; Gulino, D. A. *J. Vac. Sci. Technol. A* **1985**, *3*, 681.
(13) Yamamoto, K.; Ichikawa, Y.; Nakayama, T.; Tawada, Y. *Jpn. J. Appl. Phys.* **1988**, *27*, 1415.
(14) Koidl, P.; Wild, C.; Dischler, B.; Wagner, J.; Ramsteiner, M. *Mater. Sci. Forum* **1989**, *52/53*, 41.
(15) Dworschak, W.; Kleber, R.; Fuchs, A.; Scheppat, B.; Keller, G.; Jung, K.; Erhardt, H. *Thin Solid Films* **1990**, *189*, 257.
(16) Tyczkowski, J.; Pietrzyk, B.; Szymanowski, H. J. *J. Chem. Vap. Depos.* **1996**, *4*, 261.
(17) Buckley, R. G.; Moustakas, T.; Ye, L.; Varon, J. *J. Appl. Phys.* **1989**, *66*, 3595.
(18) Adamopoulos, G.; Gilkes, K. W. R.; Robertson, J.; Conway, N. M. J.; Kleinsorge, B. Y.; Buckley, A.; Batchelder, D. N. *Diamond Relat. Mater.* **1999**, *8*, 541.
(19) Gilkes, K. W. R.; Sands, H. S.; Batchelder, D. N.; Robertson, J.; Milne, W. I. *Appl. Phys. Lett.* **1997**, *70*, 1980.
(20) Gilkes, K. W. R.; Sands, H. S.; Batchelder, D. N.; Milne, W. I.; Robertson, J. *J. Non-Cryst. Solids* **1998**, *227/230*, 612.
(21) Shi, J. R.; Shi, X.; Sun, Z.; Lau, S. P.; Tay, B. K.; Tan, H. S. *Diamond Relat. Mater.* **2001**, *10*, 76.
(22) Schwan, J.; Ulrich, S.; Batori, V.; Ehrhardt, H.; Silva, S. R. *J. Appl. Phys.* **1996**, *80*, 440.
(23) Chen, C. L.; Lue, J. T. *J. Non-Cryst. Solids* **1996**, *194*, 93.
(24) Hong, J.; Goullet, A.; Turban, G. *Thin Solid Films* **1999**, *352*, 41.
(25) Lejeune, M.; Duranh-Drouhin, O.; Henocque, J.; Bouzerar, R.; Zeinert, A.; Benlahsen, M. *Thin Solid Films* **2001**, *389*, 233.
(26) Matsunuma, S. *Thin Solid Films* **1997**, *306*, 17.
(27) Lannin, J. S. *J. Non-Cryst. Solids* **1992**, *141*, 233.
(28) Compagnini, G.; Foti, G. *Nucl. Instr. Methods Phys. Res. B* **1997**, *127/128*, 639.

carbon−germanium films.[29,30] From these data, one can readily notice that the center of the peak shifts from 1400 to approximately 1500 cm^{-1} as the carbon contents in the film increases from 2.4 at. % (below which this peak is not present)[30] to pure carbon films.[27,28] It is suggested that the origin of the peak (sometimes called the amorphous C band)[30] can be connected with predominantly sp^2-bonded carbon domains that are, however, devoid of the graphitic structure.[29] This is confirmed by the annealing processes, creating a change in the film from the "pure" amorphous structure (with sp^2 sites) to the graphite-like structure, which is reflected by changes in the Raman spectra: the amorphous C peak disappears, and G and D peaks occur.[27,30]

It has been found that Raman spectroscopy is also a very helpful tool to study germanium structures. The bulk unstrained Ge crystals (cubic arrangement) are manifested in Raman spectra by a single symmetric peak centered at 300.5 cm^{-1} with a full width at half-maximum (fwhm) of 2.7 cm^{-1}.[31] Strain of the material causes a slight shift of the peak position.[32] In the case of nanocrystalline germanium, the average particle size can be determined from the peak fwhm. The basis for this estimation comes from phonon localization within nanometer-sized crystallites, which results in partial breakdown of the Raman selection rule and hence causes peak broadening.[33,34]

Smith and co-workers[35,36] were the first to obtain Raman spectra of amorphous germanium (a-Ge). Since that time a-Ge (both non- and hydrogenated) has been extensively investigated by this technique.[27,37−40] According to theoretical calculations,[41] the phonon density of states, as measured by Raman scattering, consists of four main peaks corresponding with TO-like (transverse−optic), LO-like (longitudinal−optic), LA-like (longitudinal−acoustic), and TA-like (transverse−acoustic) modes (in analogy with the vibrational density of states in a germanium crystal), which are positioned at approximately 275, 220, 160, and 80 cm^{-1}, respectively. Analysis of the TO and TA bands (mainly the fwhm and position of the TO peak and the ratio of the TA to TO intensities) gives information about the degree of disorder in the films (which can be expressed by the root-mean-square (rms) bond angle deviation, $\Delta\theta$)[42] as well as enables us to draw a conclusion on the nanostructure of the germanium films.[27,39]

Recently, investigations on carbon−germanium films performed by Raman spectroscopy have been also reported. The films were fabricated by a variety of techniques including rf cosputtering of germanium and carbon in argon (plus hydrogen) plasma,[43,44] dc magnetron sputtering in argon plasma,[45,46] rf magnetron sputtering of Ge in plasma generated in a mixture of methane, hydrogen, and argon,[47] and molecular beam epitaxy (MBE).[30,48] In all the cases the Raman spectra reveal two well-separated regions that can be attributed to Ge−Ge (50−350 cm^{-1}) and C−C (1200−1800 cm^{-1}) modes. In general, however, there is no evidence of any band related to Ge−C bonds. Such a very weak band at 530 cm^{-1}, apart from those related to Ge−Ge and C−C bonds, has been identified only for the epitaxial films with low carbon concentration (≤7%).[48] These results are evidently indicative of the fact that the carbon−germanium films are a kind of a composite amorphous material containing both carbon and germanium fractions. Jacobsohn et al.[45] have suggested that carbon and germanium atoms are segregated into distinct amorphous domains with their size being on the order of a few nanometers.

Of importance is the observation that after annealing of the carbon−germanium films at high temperature the amorphous germanium agglomerates can transform to crystalline form (a well-shaped peak at 300 cm^{-1} occurs).[46] The annealing can also produce a major change in the carbon region of the spectra (similarly as for carbon films). The D and G bands occur, indicating that the graphitic domains are formed either from the "pure" amorphous carbon structure (the amorphous C peak vanishes)[30] or sp^3 carbon structure.[46] In the case when the D and G peaks already exist (before annealing), they become more intense, which also demonstrates the creation of additional graphitic domains in the films.[44]

If we consider the structure of germanium domains in the carbon−germanium films, we have to take into account not only 3D agglomerates but also chainlike systems. An appropriate model for such systems are polygermanes that have been recently investigated by Raman spectroscopy.[49,50] It has been found that the intense lines of the stretching vibrations of the main germanium chain (−Ge−Ge−) emerge at the region of 200−350 cm^{-1}, the same range in which the lines stemming from amorphous or crystalline 3D germanium domains are observed. Additionally, in the case of polygermanes the Ge−C bonds are readily identified by bands at 550−650 cm^{-1}.

a-Ge_XC_Y:H films plasma deposited from a single organogermane precursor and fabricated in two differ-

(29) Long, N. J.; Trodahl, H. J. *J. Appl. Phys.* **1990**, *67*, 1753.
(30) Yang, B. K.; Krishnamurthy, M.; Weber, W. H. *J. Appl. Phys.* **1997**, *82*, 3287.
(31) Kobayashi, T.; Endoh, T.; Fukuda, H.; Nomura, S.; Sakai, A.; Ueda, Y. *Appl. Phys. Lett.* **1997**, *71*, 1195.
(32) Evangelisti, F.; Garozzo, M.; Conte, G. *J. Appl. Phys.* **1982**, *53*, 7390.
(33) Fujii, M.; Hayashi, S.; Yamamoto, K. *Jpn. J. Appl. Phys.* **1991**, *30*, 687.
(34) Choi, W. K.; Ng, V.; Ng, S. P.; Thio, H. H.; Shen, Z. X.; Li, W. S. *J. Appl. Phys.* **1999**, *86*, 1398.
(35) Smith, J. E. J.; Brodsky, M. H.; Crowder, B. L.; Nathan, M. I.; Pinczuk, A. *Phys. Rev. Lett.* **1971**, *26*, 642.
(36) Smith, J. E. J. *J. Non-Cryst. Solids* **1972**, *8/10*, 179.
(37) Lannin, J. S.; Maley, N.; Kshirsagar, S. T. *Solid State Commun.* **1985**, *53*, 939.
(38) Maley, N.; Lannin, J. S. *Phys. Rev. B* **1987**, *35*, 2456.
(39) Fortner, J.; Yu, R. Q.; Lannin, J. S. *Phys. Rev. B* **1990**, *42*, 7610.
(40) Chiussi, S.; González, P.; Serra, J.; León, B.; Pérez-Amor, M. *Appl. Surf. Sci.* **1996**, *106*, 75.
(41) Alben, R.; Weaire, D.; Smith, J. E. J.; Brodsky, M. H. *Phys. Rev. B* **1975**, *11*, 2271.
(42) Tsu, R.; Gonzalez-Hernandez, J.; Pollack, F. H. *Solid State Commun.* **1985**, *54*, 447.
(43) Vilcarromero, J.; Marques, F. C.; Andreu, J. *J. Non-Cryst. Solids* **1998**, *227/ 230*, 427.
(44) Vilcarromero, J.; Marques, F. C. *Thin Solid Films* **1999**, *343/ 344*, 445.
(45) Jacobsohn, L. G.; Freire, F. L. J.; Mariotto, G. *Diamond Relat. Mater.* **1998**, *7*, 440.
(46) Mariotto, G.; Vinegoni, C.; Jacobsohn, L. G.; Freire, F. L. J. *Diamond Relat. Mater.* **1999**, *8*, 668.
(47) Kumeda, M.; Masuda, A.; Shimizu, T. *Jpn. J. Appl. Phys.* **1998**, *37*, 1754.
(48) Weber, W. H.; Yang, B. K.; Krishnamurthy, M. *Appl. Phys. Lett.* **1998**, *73*, 626.
(49) Bukalov, S. S.; Leites, L. A. *Proc. SPIE* **2000**, *4069*, 2.
(50) Leites, L. A.; Bukalov, S. S. *J. Raman Spectrosc.* **2001**, *32*, 413.

ent forms (a-semiconductor and a-insulator), to our knowledge, never before were investigated by Raman spectroscopy. In this paper such investigations are presented. On their basis, as well as taking into account measurements of dc electrical conductivity, the differences in chemical structure of the films prepared under various conditions are discussed. A role played by the carbon network in this process is especially considered.

Experimental Procedures

Thin a-Ge_XC_Y:H films were produced from tetramethylgermane (TMGe) by plasma-enhanced chemical vapor deposition in the three-electrode reactor worked at the audio frequency (af) range.[2] In the reactor a small electrode, on which samples are prepared, is placed horizontally between two main perpendicular electrodes maintaining a glow discharge. The small electrode is coupled with the powered main electrode by a variable capacitor. The capacitance controls the negative amplitude of af voltage, $V_{(-)}$, measured on the small electrode with respect to the grounded electrode, and in consequence controls the ion impact energy. The negative amplitude, $V_{(-)}$, which was the only operational parameter in these studies, was changed in the range of 0−1200 V. For $V_{(-)} < 450$ V and $V_{(-)} > 450$ V, insulating (a-I) and semiconducting (a-S) films were fabricated, respectively. The deposition rate at the transition region, i.e., for 400 V $< V_{(-)} <$ 500 V, is approximately 1.1 nm/ s for both types of films.

The films were deposited on silicon (for Raman measurements) or glass (for electrical measurements) substrates from either pure TMGe vapor or its mixture with argon. In the latter case the TMGe concentration was 50 mol %. The reactor worked at a frequency of 20 kHz and with a power of approximately 50 W supplied to the system. Before every deposition the reactor was evacuated down to 0.1 Pa, and then the stationary flow of 11 sccm (TMGe or the mixture of TMGe with Ar) and the initial pressure of 13.0 Pa were established. The temperature of the substrate was approximately 380 K during the deposition.

Film thickness (about 1 μm) was measured by a Rudolf 431A null ellipsometer working at an incident light wave of 632.8 nm.

The Raman spectra were obtained using a Jobin Yvon Raman spectrometer T64000, equipped with a microscope. As a source of light an argon laser (λ = 514.5 nm and power ca. 200 mW) was used. All measurements were done at room temperature and the integration time for every single spectrum was equal to 120 min. For every kind of material the measurement was realized at eight different spots to ascertain the reproducibility of the results.

Some of the investigated samples were subjected to modification by an excimer laser beam. The modification was performed under a nitrogen pressure of 0.3 MPa. The laser power and the pulse duration were 120 mJ and 20 ns, respectively.

Measurements of dc electrical conductivity were carried out on samples in sandwich geometry (for a-I films) and in coplanar geometry (for a-S films). For the sandwich geometry, the films were deposited on the glass substrates with a thermally evaporated gold strip forming the bottom electrodes. Gold top electrodes were evaporated perpendicularly to the bottom metal strips. The active electrode area was 4.0 mm^2. The coplanar geometry was formed by two parallel gold strips (1.0 mm apart and 10 mm long) evaporated on the film. Current−voltage−temperature dependences were measured in a vacuum (0.1 Pa) using an APD Cryogenic helium system working in the range of 10−450 K and a Keithley 6517 programmable electrometer equipped with a voltage source. The specific conductivity was calculated from ohmic parts of the current−voltage characteristics.

Results

Figure 1 presents representative Raman spectra for all types of a-Ge_XC_Y:H films investigated in this work.

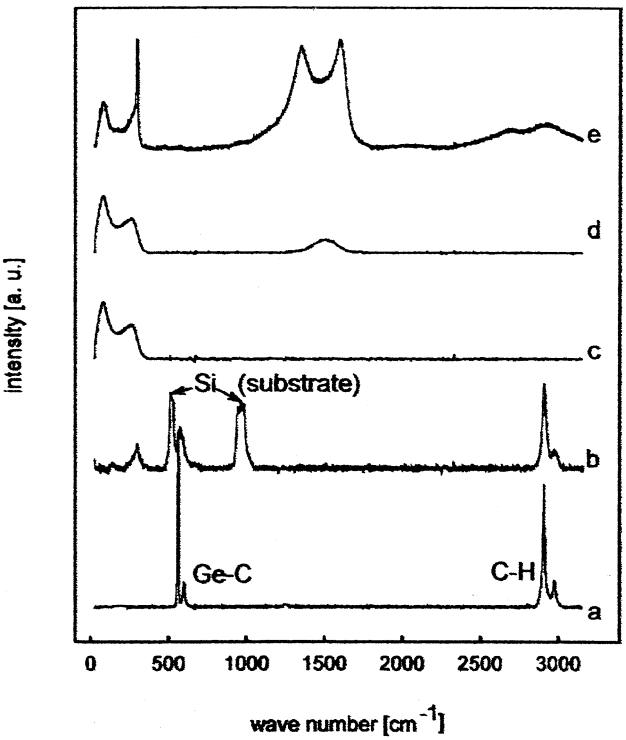

Figure 1. Raman spectra for (a) tetramethylgermane (TMGe) and a-Ge_XC_Y:H films: (b) a-I film, (c) a-S film deposited from pure TMGe, (d) a-S film deposited from TMGe−Ar mixture, and (e) a-S film after excimer laser treatment.

For comparison, a spectrum of liquid TMGe is also added (spectrum a). The spectra b and c are typical for the a-I and a-S films deposited from pure TMGe (without Ar) at $V_{(-)} < 450$ V and $V_{(-)} > 450$ V, respectively. As one can see, in both cases no signals in the carbon region (1200−1800 cm^{-1}) are visible. To verify the relation between the carbon network and the electronic properties of the films, some amount of sp^2 states was created in the a-S films by the deposition from the mixture of TMGe and Ar. As was mentioned in the Introduction, the formation of a-Ge_XC_Y:H films in the three-electrode reactor strongly depends on the ion bombardment process. In deposition from pure TMGe (without Ar), a main role in the process is played by hydrogen ions (H^+). It is known, however, that Ar^+ ions destroy the growing film and weaken the bonds more effectively than H^+ ions of the same energy.[23] According to the expectation, more drastic changes are observed in the chemical structure of the films deposited from TMGe and Ar compared to those obtained under the same conditions from pure TMGe. It is manifested by a band that emerges in the carbon region (spectrum d). Further changes in the carbon structure of the films were generated by a postdeposition treatment carried out by the excimer laser pulses (spectrum e).

More thorough analysis of the bands in the carbon region shows that in the case of the films deposited from the TMGe and Ar mixture only a single broad (fwhm ≈ 150 cm^{-1}) Gaussian peak exists, with a maximum at 1503 cm^{-1} (Figure 2). It lies between typical locations of the graphite D and G bands and cannot be fitted as a linear combination of them. Consequently, the peak is attributed to the amorphous C band. On the other hand, the carbon part of the spectrum for the laser-treated films is more complex (Figure 3). It has been

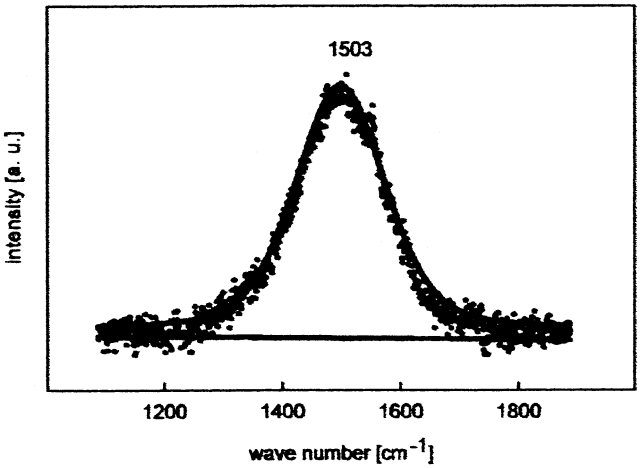

Figure 2. Raman spectrum in the carbon region for a-S film deposited from TMGe−Ar mixture (points, measurement results; line, Gaussian approximation of the band).

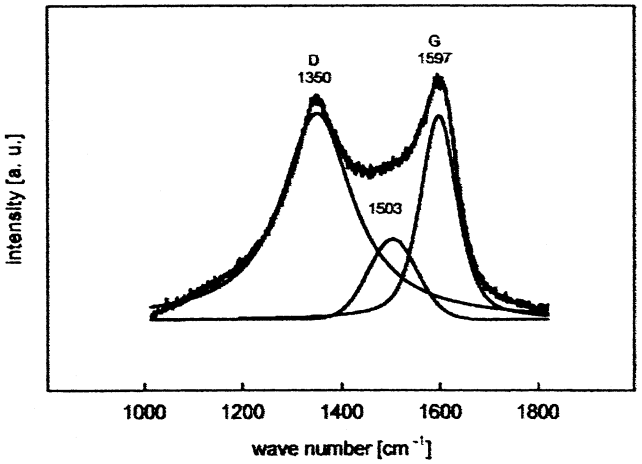

Figure 3. Raman spectrum in the carbon region for a-S film deposited from the TMGe−Ar mixture, after excimer laser treatment (peaks separated by a numerical peak-fitting procedure are shown).

Table 1. Parameters of Raman Peaks in the Carbon Region for a-S Films Deposited from TMGe−Ar Mixture, after Excimer Laser Treatment

Raman band	peak position (cm^{-1})	fwhm (cm^{-1})	relative area (au)
D	1350	190	68.3
C	1503	109	11.0
G	1597	87	20.7

analyzed according to a numerical peak-fitting algorithm (PeakFit software by Jandel), in which Gaussian and Gaussian−Lorentzian peak functions were used. The peaks were scaled in a way to give a total area under the spectrum equal to 100. Three peaks are separated in this case. Their parameters as the maximum position, fwhm, and integrated area are collected in Table 1. It is evident that the peaks at 1350 and 1597 cm^{-1} are the graphite D and G bands, respectively. Moreover, the amorphous C band (1503 cm^{-1}) is also present, although its integrated area amounts only to about 11% of the whole sp^2 carbon signal.

As far as the germanium region of the spectra (50−350 cm^{-1}) is concerned, its bands have been analyzed analogously to the numerical method mentioned above. The results of such a numerical analysis for the a-I film,

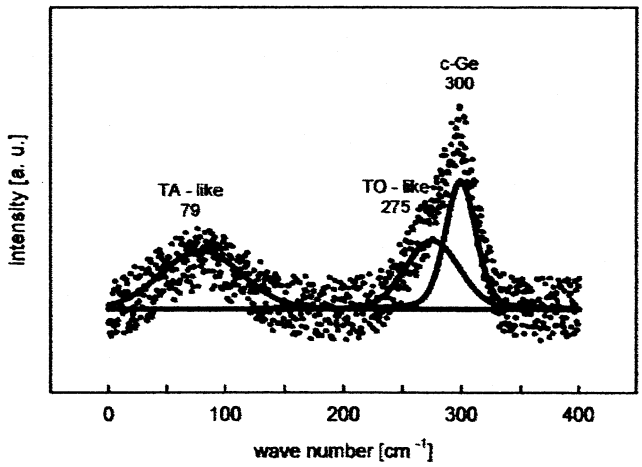

Figure 4. Raman spectrum in the germanium region for a-I film (peaks separated by a numerical peak-fitting procedure are shown).

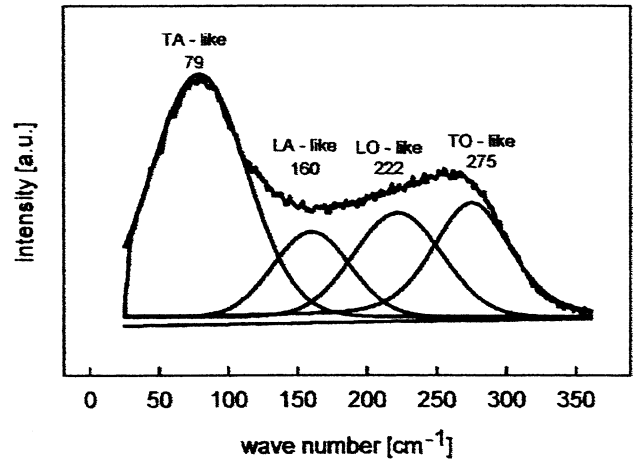

Figure 5. Raman spectrum in the germanium region for a-S film (peaks separated by a numerical peak-fitting procedure are shown).

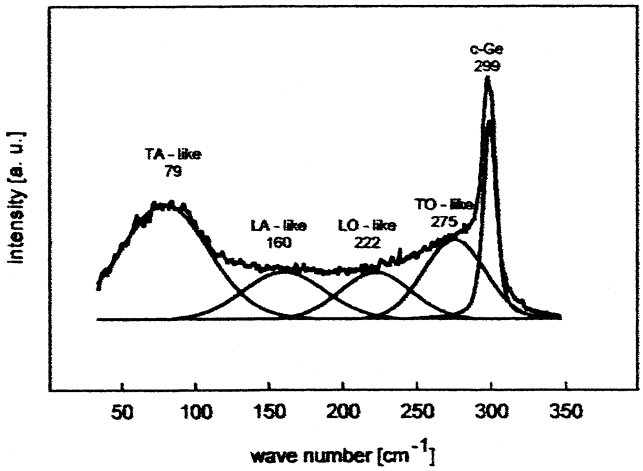

Figure 6. Raman spectrum in the germanium region for a-S film after excimer laser treatment (peaks separated by a numerical peak-fitting procedure are shown).

a-S film, and a-S film after laser treatment are shown in Figures 4, 5, and 6, respectively. The germanium part of the spectra for the a-S films deposited from both pure TMGe and the TMGe + Ar mixture is practically identical. The parameters describing the separated peaks for all the spectra are presented in Table 2. It

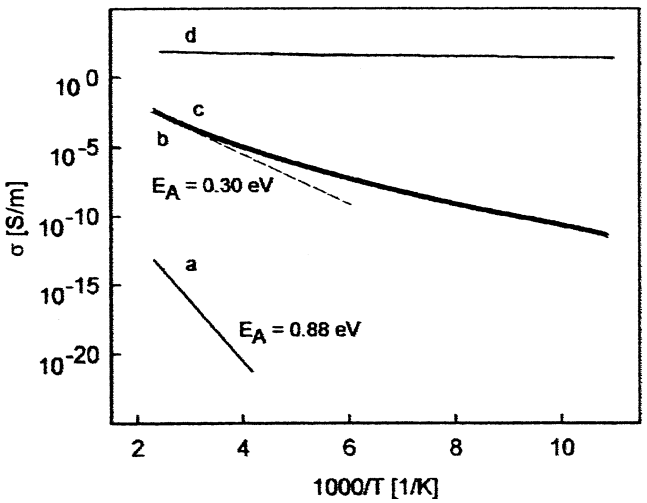

Figure 7. Dependence of the electrical conductivity, σ, on reciprocal temperature for (a) a-I film, (b) a-S film deposited from pure TMGe, (c) a-S film deposited from TMGe−Ar mixture, and (d) a-S film deposited from TMGe−Ar mixture, after excimer laser treatment.

Table 2. Parameters of Raman Peaks in the Germanium Region for Insulating and Semiconducting a-Ge_XC_Y:H Films

Raman band	peak position (cm^{-1})	fwhm (cm^{-1})	relative area (au)
	a-I Films		
TA-like	79	80	39.8
TO-like	275	47	28.5
Ge-chain	300	31	31.7
	a-S Films		
TA-like	79	78	40.8
LA-like	160	95	17.5
LO-like	222	88	23.3
TO-like	275	68	18.4
	a-S Films after Laser Treatment		
TA-like	79	62	36.6
LA-like	160	71	16.5
LO-like	222	47	9.2
TO-like	275	49	23.4
c-Ge	299	10	14.3

should be added that the measurements for a-I type material are more difficult to realize than those for the a-S type due to the much lower intensity of the Raman signals. Also, much lower absorption of the exciting light (514.5 nm) is observed in the a-I samples. That is why the Si lines (512 and 950 cm^{-1}) from silicon substrate are also visible (Figure 1, spectrum b).

In general, the analysis of the germanium region of all investigated spectra shows that in all these cases typical a-Ge bands, such as TO-like, LO-like, LA-like, and TA-like, can be distinguished. Due to the low intensity of the Raman signal and its noise for a-I samples, only two main a-Ge bands (TA-like and TO-like) were used to fit the spectrum (Figure 4). In this case, however, like for the a-S samples after laser-treatment (Figure 6), an additional band at approximately 300 cm^{-1} appears.

For characterization of the electronic properties of the films under discussion, the temperature dependence of the conductivity, σ, was measured (Figure 7). As one can see, three groups of films can be distinguished: those with low σ and activation energy $E_A \approx 0.9$ eV, which was calculated from the slope of curve a (a-I films); those with high σ and an activation energy near room temperature $E_A \approx 0.3$ eV [a-S films deposited from both pure TMGe (curve b) and TMGe + Ar (curve c)]; and those with very high values of conductivity practically independent of temperature (a-S films modified by the excimer laser pulses, curve d). Differences in σ between the first and the second group (at room temperature, T_{room}, it is approximately 14 orders of magnitude) represents the a-I−a-S transition −the process under investigations in this paper. The further increase in σ (visible between the second and the third group, approximately 6 orders of magnitude at T_{room}) reveals quite a different process created by the laser treatment, which effectively affects the electronic structure of the a-S films.

Discussion

Carbon Structure. The fact that the carbon content in the a-Ge_XC_Y:H films, for both a-I and a-S, is very high (80−85 mol %)[2] and no Raman signals of sp^2 carbon are observed for these films when they are deposited from pure TMGe (Figure 1, spectra b and c) is indicative of a carbon network only tetrahedrally (sp^3) bonding. In the case of a-I films, some amount of $-CH_3$ groups, testifying to the polymer-like character of these films, is identified by the lines in the region of 2800−3000 cm^{-1} [by analogy with the spectrum of TMGe (Figure 1, spectrum a)]. On the other hand, for the a-S material (where bands at 2800−3000 cm^{-1} are absent) one can assume a more cross-linking three-dimensional carbon structure realized by C−C (sp^3) bonds. It is very striking that although we do not see any sp^2 sites in the a-S films, nevertheless the drastic difference in σ between a-I and a-S is observed (Figure 7, curves a and b). Moreover, the creation of sp^2 sites in the amorphous carbon network of a-S films, caused by the addition of argon to TMGe during deposition, does not change the σ of these films at all (Figure 7, curve c). These observations lead to an important conclusion, namely that the carbon matrix does not determine here the electronic structure and therefore it is not responsible for the a-I−a-S transition in the a-Ge_XC_Y:H films under discussion.

The influence of the carbon structure on the electronic properties of the films can be observed, but only when the graphitization process proceeds in the material. Such a process is generated by the excimer laser treatment. As one can see in Figure 3, the strong D and G graphite bands occur in the spectrum. Taking into account that their intensities are almost the same ($I_D/I_G \approx 1$) and the G band fwhm is equal approximately to 90 cm^{-1}, it is possible to state that the graphite phase is mostly dominated by small aromatic clusters with cluster sizes lower than 1 nm.[22] In this case, a subsequent increase in σ (approximately 6 orders of magnitude at T_{room}) and changes in the current−temeperature dependence [from thermally activated ($E_A \approx 0.3$ eV) to nonactivated conductivity] take place (Figure 7). These results are evidently indicative of a change in the charge carrier transport mechanism in the a-S films. This is, however, an absolutely different effect from that classified as the a-I−a-S transition. The fact that sp^2 sites are able to modify the electronic structure of the a-Ge_XC_Y:H films, but in another way than in the

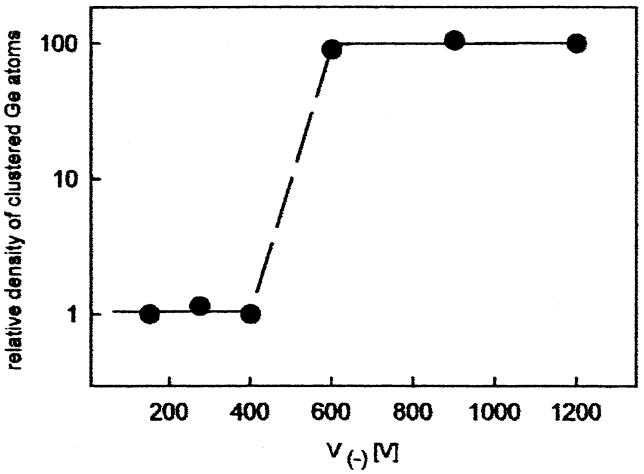

Figure 8. Relative density of clustered Ge atoms in a-Ge_XC_Y:H films as a function of the $V_{(-)}$ parameter controlling the deposition of these films.

a-I−a-S transition, confirms the independence of this transition from the "pure" carbon structure.

Germanium Structure. Taking into consideration the discussion presented above, the search for a reason for the a-I−a-S transition effect on the molecular level should be focused on germanium atoms and the role they play in the a-Ge_XC_Y:H films. It is visible that for both a-I and a-S films the bands of amorphous germanium are present (Figures 4 and 5). Beyond a doubt this is indicative of the existence of a-Ge clusters in the films. One sees at once, however, that the signals for a-I are much lower than those for a-S. By comparing the integrated areas of Ge bands (TA-like and TO-like) measured for the both materials at the same experimental adjustments, it has been found that signals in the case of a-S are about 1 order of magnitude stronger than that for a-I. To compare the Ge-cluster-fraction density, we have to take also into account different values of the absorption coefficient, α, for a-I and a-S at 514.5 nm. For the a-S films $\alpha = 2.5-3.6 \times 10^6$ m^{-1} (depending on $V_{(-)}$),[1] and one can estimate that the effective thickness ($1/\alpha$) is approximately 280−400 nm. On the other hand, in the case of a-I, where $\alpha \approx 10^5$ m^{-1},[1] and hence $1/\alpha \approx 10^4$ nm, laser light can penetrate the full thickness of the films ($d \approx 1.5 \times 10^3$ nm) practically without its intensity loss. Then the laser beam is reflected from the silicon substrate [Si lines are visible in the Raman spectrum (Figure 1, spectrum b)] and once again passes through the films. Thus, the a-I films, with an effective thickness of approximately 3×10^3 nm, should be considered as responsible for the observed Raman signal. It is about 10 times as thick as the effective layer of a-S. Although at this stage of investigations we cannot precisely estimate the absolute number and size of the a-Ge clusters, it is evident that the density of Ge atoms in clusters is approximately 2 orders of magnitude higher for the a-S films than for the a-I films. The rest of the Ge atoms in the a-I films are molecularly dispersed, which is confirmed by the band at 570 cm^{-1} attributed to Ge−C bonds (Figure 1). The results of calculation of the relative density of clustered Ge atoms for all investigated films are presented in Figure 8.

More thorough analysis of the a-Ge bands gives information about the degree of disorder in Ge clusters. Taking values of fwhm for the TO-like peak presented in Table 2, the rms bond angle deviation, $\Delta\theta$, has been estimated according to the method described by Tsu at al.[42] The values of $\Delta\theta$ are approximately 12.0°, 8.0°, and 8.5° for a-S, a-I, and a-S after laser treatment, respectively. As one can see, the molecular structure of a-Ge clusters in the a-S films is more disordered than that of the a-I material. This effect is most probably connected with a stress induced in a-Ge clusters by the more cross-linked carbon matrix, including these clusters in the case of a-S films. After excimer laser treatment, a structural relaxation of a-Ge clusters in the a-S films takes place and the decrease in $\Delta\theta$ from 12.0° to 8.5° is observed.

Finally, some attention should be also paid to the band at about 300 cm^{-1} that is recorded as a very weak signal for the a-I films (Figure 4) and a relatively strong signal for the a-S films after laser treatment (Figure 6). In the latter case it is unquestionable that the band is related to Ge nanocrystals that are created by energy supplied by the laser pulses. The presence of the c-Ge form in the film is confirmed by the electron diffraction measurements revealing a typical pattern for crystalline germanium.[51] Taking the fwhm value of the 300 cm^{-1} band from Table 2 (10 cm^{-1}), an average size of the Ge nanocrystals has been estimated according to Choi et al.[34] It is approximately 6.0 nm. If we assume that the Ge nanocrystals are formed by structural relaxation of the a-Ge clusters, we can conclude that the size of these clusters in the a-S films should be also on the order of a few nanometers.

The origin of the weak 300 cm^{-1} band in the a-I films is more difficult to explain. The very high fwhm value in this case (31 cm^{-1}) (Table 2) as well as a complete lack of the characteristic electron diffraction pattern for germanium crystalline form[5] exclude rather the possibility that the band stems from Ge nanocrystals. Recently, it has been found, however, that the Ge−Ge stretching vibrations for polygermanes can also give bands in the region of 300 cm^{-1}.[49,50] At this stage it seems to be more reasonable to attribute the 300 cm^{-1} band in the a-I material to short germanium chains.

Summarizing, one can state that in the a-I films, apart from a great amount of Ge atoms that are molecularly dispersed, a very low density of 3D (clusters) and 2D (chains) systems exists. On the other hand, in the case of the a-S films, the vast majority of Ge atoms are in the form of a-Ge clusters. The excimer laser treatment causes a transformation of some part of the a-Ge clusters to Ge nanocrystals. It should be emphasized that the transition from the a-I material with a very low density of a-Ge clusters to the a-S material characterized by a very high density of clusters proceeds rapidly when the negative amplitude surpasses $V_{(-)} =$ 450 V (Figure 8). In other words, the a-I−a-S transition takes place when the impact energy of ions bombarding the growing film exceeds some critical value. This energy is sufficient to activate the separation process of an amorphous germanium phase in the deposited a-Ge_XC_Y:H films. This is thermodynamically justified in the light of the fact that the mutual solid solubility of Ge and C is negligible in their mixture in a state of

(51) Tyczkowski, J.; Kazimierski, P.; Hatanaka, Y.; Aoki, T.; Nakanishi, Y. In preparation.

equilibrium.[52] As a result, a high density of a-Ge clusters occurs in the film. The clusters play a crucial role in the formation of an amorphous semiconductor network characterized by extended states, in contradistinction to the a-I material, in which only localized states exist. It was suggested in previous papers,[1,3,6−8] based on earlier discussions,[10,53] that the transition occurs when some critical strength of disorder in the deposited film is attained and in the place of a-I, in which all states are localized, a new structure of a-S with extended states is created. The results obtained by means of Raman spectroscopy confirm and develop this conception in the case of the a-Ge_XC_Y:H films. However, to better understand the molecular and electronic structure of the semiconducting phase constructed from the a-Ge clusters, further investigations, among others of ac conductivity, will be performed.

Summary

Although the drastic changes in electronic properties could be observed in a-Ge_XC_Y:H films deposited in the three-electrode af plasma reactor when the negative amplitude of af voltage, $V_{(-)}$, exceeded the value of 450 V, the investigations performed by XPS and IR spectroscopies for both types of films (for $V_{(-)} < 450$ V and $V_{(-)} > 450$ V) did not reveal any changes that could explain such a transition in the electronic structure (a-I−a-S transition). Recently, significant progress toward a solution to this problem has been made by our studies carried out by Raman spectroscopy, which enables us to distinguish and analyze carbon and germanium nanostructures. It has been found that, against expectations, the carbon matrix does not determine the electronic properties of the a-Ge_XC_Y:H films under discussion and therefore it is not responsible for the a-I−a-S transition. In both a-I and a-S films, no sp^2 sites have been seen. Nevertheless, a rapid change in their electrical conductivity, σ (approximately 14 orders of magnitude at T_{room}), is observed. Moreover, the creation of sp^2 sites in the amorphous carbon network of a-S films, caused by the addition of argon to TMGe during deposition, does not change the σ of these films at all. Such changes can be created only when a graphite-like phase occurs in the films, for instance, as a result of the excimer laser treatment. However, these changes in the electronic properties of the films are quite different from those responsible for the a-I−a-S transition.

On the other hand, it has been found that the a-I and a-S films drastically differ in the character of germanium nanostructure from one another. In the a-I films, apart from a great amount of Ge atoms that are molecularly dispersed, a very low density of 3D (clusters) and 2D (chains) systems exists, whereas in the case of the a-S films, the vast majority of Ge atoms is in the form of a-Ge several-nanometer-sized clusters. It is suggested that these clusters play a crucial role in the formation of an amorphous semiconductor network, which is responsible for the a-I−a-S transition. The drastic increase in the cluster density occurs when the impact energy of ions bombarding the growing film exceeds a value sufficient to activate the separation process of the amorphous germanium phase in the deposited a-Ge_XC_Y:H films. In our case this value is attained for $V_{(-)} \approx 450$ V.

Further investigations should be focused on understanding the molecular and electronic structures of the semiconducting phase constructed from the a-Ge clusters in the amorphous semiconducting a-Ge_XC_Y:H films. It seems to be also very important to investigate by Raman spectroscopy other types of plasma deposited films, such as a-Si_XC_Y:H, a-Sn_XC_Y:H, and a-Pb_XC_Y:H, in which the a-I−a-S transition is observed.

Acknowledgment. One of us (J.T.) expresses his gratitude to the Japan Society for the Promotion of Science for a financial support of his stay in the Research Institute of Electronics in Hamamatsu (Japan), where the excimer laser treatment experiments were perfomed.

CM020428S

(52) Scase, R. I.; Slack, G. A. *J. Chem. Phys.* **1959**, *30*, 1551.
(53) Adler, D. *Solar Energy Mater.* **1982**, *8*, 53.